Passive tracer transport relevant to the TRACE A experiment

JOURNAL OF GEOPHYSICAL RESEARCH, VOL. 101, NO. D19, PAGES 23,889–23,907, OCTOBER 30, 1996

Passive tracer transport relevant to the TRACE A experiment

T. N. Krishnamurti,[1] M. C. Sinha,[1] M. Kanamitsu,[2] D. Oosterhof,[1] H. Fuelberg,[1]
R. Chatfield,[3] D. J. Jacob,[4] and J. Logan[4]

Abstract. This paper explores some of the mechanisms governing the accumulation of passive tracers over the tropical southern Atlantic Ocean during the northern hemisphere fall season. There has been a pioneering observation regarding ozone maxima over the South Atlantic during austral spring. The understanding of the formation of this maxima has been the prime motivation for this study. Using a global model as a frame of reference, we have carried out three kinds of experiments during the period of the Transport and Atmospheric Chemistry Near the Equator—Atlantic (TRACE A) project of 1992. The first of these is a simple advection of total ozone (a passive tracer) in time using the Florida State University global spectral model. Integration over the period of roughly 1 week showed that the model quite closely replicates the behavior of the observed total ozone from the total ozone mapping spectrometer (TOMS). This includes many of the changes in the features of total ozone over the tropical and subtropical region of the southern Atlantic Ocean. These studies suggest a correlation of 0.8 between the observed ozone over this region and ozone modeled from "dynamics alone," i.e., without recourse to any photochemistry. The second series of experiments invoke sustained sources of a tracer over the biomass burn region of Africa and Brazil. Furthermore, sustained sources were also introduced in the active frontal "descending air" region of the southern hemisphere and over the Asian monsoon's east-west circulation. These experiments strongly suggest that air motions help to accumulate tracer elements over the tropical southern Atlantic Ocean. A third series of experiments address what may be required to improve the deficiencies of the vertical stratification of ozone predicted by the model over the flight region of the tropical southern Atlantic during TRACE A. Here we use the global model to optimally derive plausible accumulation of burn elements over the fire count regions of Brazil and Africa to provide passive tracer advections to closely match what was observed from reconnaissance aircraft-based measurements of ozone over the tropical southern Atlantic Ocean.

1. Introduction

Since the pioneering observational studies on tropospheric ozone distribution [*Fishman*, 1994; *Fishman et al.*, 1990, 1991], the issues on the source regions have focused on the biomass burning over South America and Africa [*Fishman et al.*, 1990; *Thompson et al.*, 1993]. Fishman's original studies examined two types of satellite observations: total ozone mapping spectrometer (TOMS) for the total atmospheric column ozone and stratospheric aerosol and gas experiment (SAGE) for the stratospheric component. A list of acronyms is provided in Table 1. These studies qualitatively provided a convincing picture of a tropospheric ozone maximum, which was centered near the Greenwich meridian and roughly 10° to the south of the equator. Plate 1 from *Fishman et al.* [1990] describes the residual tropospheric ozone obtained from the subtraction of the stratospheric ozone (as measured from SAGE) from the total ozone (as measured from TOMS). This pioneering work has led to the participation of a large number of scientists in the investigation of this tropospheric anomaly over the tropical southern Atlantic Ocean.

Ozonesonde measurements of the vertical distribution at several sites provided insight into the possibility that accumulation of ozone can occur in the lower troposphere near the oceanic inversion and in the upper troposphere as well. Refinements of the early satellite measurements of total ozone [*Fishman et al.*, 1990] were provided by *Thompson et al.* [1993], who emphasized the corrections for the oceanic stratocumulus. Satellite observations suggest that the tropospheric ozone has a relative maximum during the austral spring, i.e., September and October. The atmospheric circulations over a broad-scale region covering Africa, South America, and the Atlantic Ocean were summarized by *Krishnamurti et al.* [1993]. They described the circulation climatology (i.e., monthly means) as well as the transients of this region. It was recognized that atmospheric transport processes could include possible candidates such as (1) divergent planetary east-west circulations with ascending branches in the Asian monsoon region and descending air over the tropical southern Atlantic Ocean; (2) frontal descent of the southern hemispheric air, which was shown to subsequently circulate northward in the lower troposphere, i.e., counterclockwise around transient anticyclones of the southern tropics and subtropics; (3) biomass burn elements from South America, being eventually conveyed via the westerlies near 25°S and

[1]Department of Meteorology, Florida State University, Tallahassee.
[2]National Meteorological Center, Washington, D. C.
[3]Earth System Science Division, NASA Ames Research Center, Moffett Field, California.
[4]Department of Earth and Planetary Sciences, Harvard University, Cambridge, Massachusetts.

Paper number 95JD02419.
0148-0227/96/95JD-02419$09.00

Table 1. List of Acronyms

Acronym	Definition
DU	Dobson unit
FSU	Florida State University
UV DIAL	UV differential absorption lidar
NMC	National Meteorological Center
SAGE	stratospheric aerosol and gas experiment
TOMS	total ozone mapping spectrometer
TRACE A	Transport and Atmospheric Chemistry Near the Equator—Atlantic
UTC	coordinated universal time

around transient anticyclones to the tropical southern Atlantic; (4) biomass burn elements over Brazil being conveyed to the upper troposphere by deep cumulus convection and eventually conveyed by westerlies toward the tropical southern Atlantic; (5) the easterly flow near 700 mbar can convey low-level burn elements from the interior of the biomass burn regions of Africa; and (6) the upper tropospheric near-equatorial easterly flows over Africa appear to be possible vehicles for the transport of burn elements, which has been previously carried to the upper troposphere by deep cumulus convection. The determination of reliable flow trajectories that might provide insight on the relative importance of such candidates is not a simple matter [*Pickering et al.*, 1994; *Fuelberg et al.*, this issue]. Difficulties stem from uncertainties in data coverage, analysis assimilation differences from various centers, usage of model-based data by users using alternate algorithms (different from those used by modelers), methodology, and space-time interpolations in the construction of trajectories. A nonlinear advection of passive tracers, using a fourth-order semi-Lagrangian advective scheme [*Krishnamurti et al.*, 1990] used in this study eliminates most of these difficulties.

There are important questions as to what dynamics only contributes, as compared to the contribution of the photochemistry of the biomass burn, toward the eventual pattern of the ozone accumulation over the tropical southern Atlantic Ocean. The role of the dynamics is something that we can perhaps address from our modeling capability. However, we feel that, given the half-life of the ozone, of roughly a week in the lower troposphere and roughly 3–4 weeks in the upper troposphere and stratosphere, the ad hoc nature of our approach in neglecting the contributions of photochemistry may still be quite acceptable, since we are examining periods of 6 days only. The eventual strategy of long-term transport studies would, however, require four-dimensional global models at high resolution that include photochemical history variables.

The field experiment Transport and Atmospheric Chemistry Near the Equator—Atlantic (TRACE A) was conducted over this entire region of interest during the months of September and October 1992. A chronology of the components of the experiments appears in this special issue of the *Journal of Geophysical Research* [*Bachmeier and Fuelburg*, 1995]. One purpose of this field experiment was to provide a diverse set of observations for circulation and photochemical studies toward providing an understanding of the role of biomass burning on the accumulation of the tropical tropospheric ozone over the southern Atlantic Ocean.

2. Objectives of the Present Study

The main objective of the present study is to use results from the Florida State University (FSU) global spectral models at high resolution, to investigate the relative roles of passive tracer transports based on TOMS and those based on simply modeled biomass burn patterns on the accumulation of ozone over the tropical southern Atlantic Ocean.

3. Data Sources for the Present Study

For the initial state of atmosphere, we have used the National Meteorological Center (NMC) operational level III data sets, which are based on analysis of the conventional World Weather Watch observations data, the available global data from commercial aircraft, data from ships of opportunity, the polar orbital satellite based soundings, cloud-tracked winds, and some surface buoy data from the equatorial Pacific and the southern hemisphere.

Enhanced cloud-tracked winds over the tropical Atlantic Ocean were studied. During the months of September and October 1992 an enhanced extraction of cloud motion vectors was organized by Florida State University (carried out by Jack Beven) on the National Hurricane Center's McIdas system. These data were passed on to the NMC and were assimilated in near real-time by their four-dimensional assimilation system [*Kanamitsu*, 1989] into their global analysis.

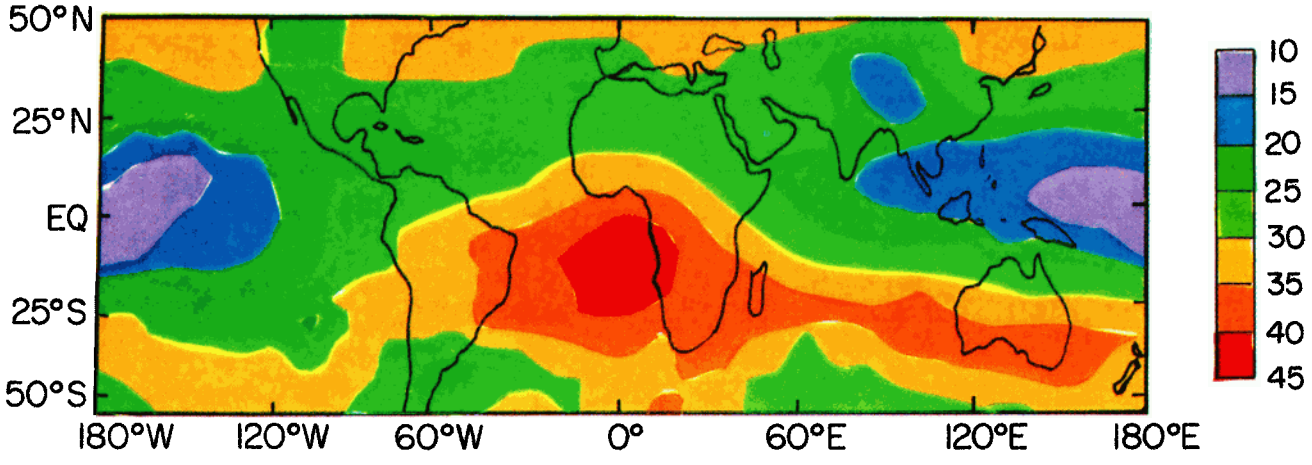

Plate 1. Distribution residual of tropospheric ozone for October determined from concurrent measurements made by the SAGE and the TOMS [adapted from *Fishman et al.*, 1990].

TRACE A dropwinsonde data from NASA's DC-8 were used. The flight tracks of the aircraft are illustrated by *Bachmeier and Fuelberg* [this issue]. The dropsonde data for the flights were incorporated into the global analysis system described above.

TOMS, the total ozone global data, for this period were provided to us by NASA Goddard. These data sets did not include the cloud correction algorithm of *Thompson et al.* [1993].

A first guess vertical distribution of ozone for the TOMS was based on *Dütsch* [1978] and *Hilsenrath et al.* [1977].

Tropopause height (pressure) data sets were obtained from the archives of the NMC.

In order to delineate the tropospheric ozone for our model-based estimates, it was necessary to perform integrations from the Earth's surface to the tropopause. For this purpose, we have resorted to the NMC's operational analysis of the tropopause pressure. We examined the tropopause analysis for the period October 12–18. Typical values of tropopause location are around 120 mbar near the Greenwich meridian and 10°S. The tropopause descends to roughly 250–300 mbar near 60°S, and the tropopause is somewhat above the 120-mbar surface over the northern summer tropics. In this study we have not addressed the specifics of tropospheric residue ozone, since such data were not available at the time of this research. Those aspects will be addressed in a future study.

4. The Global Model

The global model used in this study is identical in all respects to that used by *Krishnamurti et al.* [1989]. The characteristics of the global model are as follows: independent variables (x, y, σ, t); department variables of vorticity, divergence, surface pressure, vertical velocity, temperature, and humidity; horizontal resolution of 126 triangular waves; vertical resolution of 15 layers between roughly 30 and 1000 mbar; semi-implicit time differencing scheme; centered differences in the vertical for all variables except humidity, which is handled by an upstream differencing scheme (the humidity variables require a positive definite advective scheme); fourth-order horizontal diffusion [*Kanamitsu et al.*, 1983]; Kuo-type cumulus parameterization [*Krishnamurti et al.*, 1983]; shallow convection [*Tiedke*, 1984]; dry convective adjustment; large-scale condensation [*Kanamitsu*, 1975]; surface fluxes via similarity theory [*Businger et al.*, 1971]; vertical distribution of fluxes utilizing diffusive formulation, where the exchange coefficients are functions of the Richardson number [*Louis*, 1979]; longwave and shortwave radiative fluxes based on band models [*Lacis and Hansen*, 1974; *Harshvardan and Corsetti*, 1984]; diurnal cycle; parameterization of low, middle, and high clouds based on threshold relative humidity for radiative transfer calculations; surface energy balance is coupled to the surface similarity theory [*Krishnamurti et al.*, 1991]; nonlinear normal mode initialization of five vertical modes [*Kitade*, 1981].

Other aspects of global modeling entail the passive advections of ozone. For this purpose, we have designed an advection algorithm that makes use of the semi-Lagrangian conservation principle based on *Krishnamurti et al.* [1990].

5. Passive Tracer Experiments

In this section, we shall describe in sequence, the experiments based on dynamics alone, isolated source, and optimized burn.

5.1. Dynamics-Alone Experiment

Our interest lies with the issue of the contribution to the accumulation of tropical tropospheric ozone from dynamics, i.e., no photochemistry is invoked. The global model is first integrated for a period of 6 days and, using its three-dimensional motion field (u, v, $\dot{\sigma}$), the transports are next carried out by the predicted winds in order to study the time history of the passive tracer. The initial ozone is derived from the TOMS data set, which is the vertically integrated atmospheric ozone. Next we shall describe the results for an experiment that was initialized for October 12, 1992, at 0000 UTC.

The initial vertical distribution of ozone was determined from the TOMS data using the weighting function given by *Dütsch* [1978] and *Hilsenrath et al.* [1977] to get the distribution of ozone at every 50 hPa in the vertical and at every 1.25° latitude from south pole to north pole. This provided a four-dimensional global distribution of ozone, i.e., $O(\lambda, \theta, \sigma, t)$, where O is the amount of ozone, λ the longitude, θ the latitude, σ the normalized pressure coordinate in the vertical, and t the time. The distribution of the weighting functions is given in Figure 1a. Although the initial vertical distribution of ozone is a function of the imposed climatological weights initially, we noted that the model during the course of a 1 day forward integration achieves a stable and realistic three-dimensional structure that was seen from an examination of the time history of the predicted structure function (weights), $W(\theta, \sigma, t)$. Here the structure function is defined by

$$W(\theta, \sigma, t) = \frac{\int_\lambda O(\lambda, \theta, \sigma, t)\, d\lambda}{\int_0^1 \oint_u O(\lambda, \theta, \sigma, t)\, d\lambda, d\sigma}$$

These computations were carried out at the end of each day of forecast. The results for days 2, 4 and 6 are shown in Figures 1b–1d. Here we note the largest changes (i.e., adjustment in the weighting function) occur between days 0 and 1. This simply suggests that for the given global model and the prevailing four-dimensional motion field an equilibrated weighting function is realized. Of course, that weighting function is limited to what the model approximations are, and the equilibration may not reflect the details of vertical stratification generated by biomass burning. In that sense we shall regard the results from this first experiment to reflect mainly the effects of transport from dynamics alone.

Kim et al. [this issue] have proposed a new method for obtaining tropospheric ozone estimates. They invoked correction for an albedo effect in order to improve the stratospheric estimates provided by SAGE. Furthermore, they corrected for a bias in the TOMS measurements over land areas as compared to adjacent stratocumulus-covered ocean. Our estimates of TOMS have not been corrected. It would have been desirable to make corrections for the albedo and the land bias. These will be included in future studies. The heavy arrow in Figure 5 denotes a prominent divergent streamline illustrating the teleconnection between the ozone maximum and the Asian monsoon.

We make the assumption that, over a short period of the order of a week, the stratospheric changes in the ozone are small. Next we shall present the total ozone based on the TOMS data and those obtained from these global model forecasts. The period October 12–18, 1992, is considered here. The TOMS data are displayed in the top panels of Figures 2a–2l. The bottom panel shows the predicted ozone from the global model. The model's initial estimates also reflect some errors

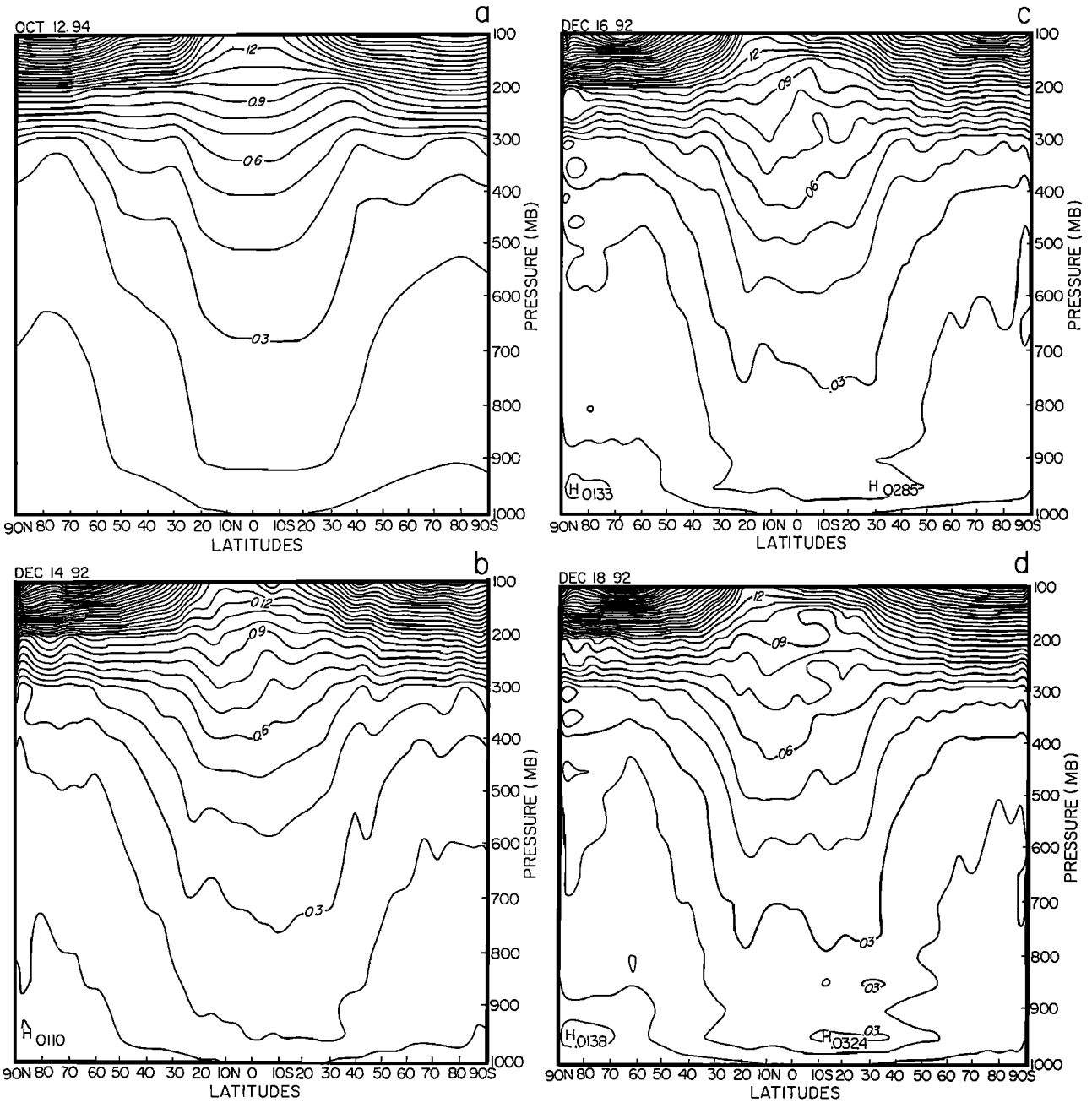

Figure 1. Tropospheric weights based on ozone structure function of *Dütsch* [1978] and *Hilsenrath et al.* [1977] and as implied by the global model.

arising from interpolation to the T126 resolution, which has a transform grid separation of roughly 80 km.

The predicted total ozone is in close agreement with the TOMS estimates throughout this 6-day period of October 12–18, 1992. If one looks at the 6-day forecast for October 18 (Figures 2k and 2l), we can see that many of the small-scale details are reasonably predicted by the global model. An axis of a sharp gradient of total ozone extends from 20°W to 10°E across 40°S. This sharp feature is related to a frontal passage, and the circulation forecasts are able to convey these ozone transports accurately. A tongue of ozone maximum enters the Indian Ocean from the southern Atlantic Ocean south of South Africa; this is another of the many features that is reasonably predicted at day 6. The 300 Dobson unit (DU) isopleth over South America reflects a southward dip near 30°S; this is also reasonably portrayed by the forecast model. Over the tropical southern Atlantic Ocean the TOMS carries a maximum value of 314 DU, whereas the predicted maximum value over this region is around 308 DU. Overall, the 6-day forecast of the distribution of ozone appears quite realistic. The high skill in the prediction of ozone distribution is also reflected in the correlation diagram (Figure 3). Here we show the correlation of the observed and the predicted ozone versus days of forecast. It may be seen from Figure 3 that the forecast skill falls to 0.6 at day 6. The errors arise from modeling approximations associated with forecast errors of the motion field and hence of the transports. The absence of photochemistry is, of course, another factor that must account for these errors, since

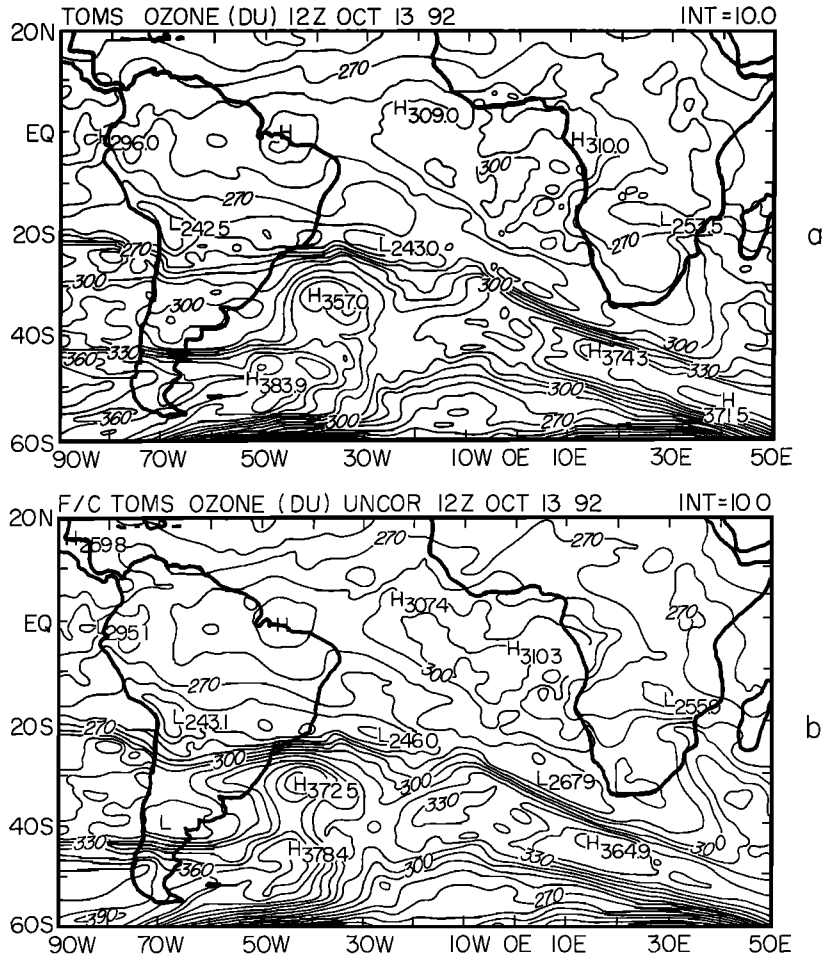

Figure 2. (a, c, e, g, i, k) Observed ozone (based on TOMS uncorrected) and (b, d, f, h, j, l) predicted ozone. Units are DU. The figures cover day 1 through day 6 of forecast between October 13 through October 18, 1992, 1200 UTC respectively.

we only include the transports of a passive tracer. *Thompson et al.* [this issue] have discussed the uncertainties of the daily total ozone (TOMS). They have also mentioned that averaged over periods of the order of a week or longer, the uncertainties as measured against dropsonde data from Brazzaville, Natal, and Ascension are reduced considerably. For this reason, we also performed a correlation of the weekly mean observed ozone (TOMS) versus the forecast ozone from the global model. That correlation over the larger TRACE A region came out to roughly 0.8. This is another measure of the success of the prediction of total ozone. It perhaps also reflects the fact that transport by dynamics alone describes a major proportion of the observed ozone. It also clearly demonstrates that the model gives good predictions, and if the proper initial distribution is known, accurate prediction of passive tracers can be made. The results presented here may, however, be sensitive to the particular choice of structure functions. Further experimentation is needed to ask what impact on the dynamics alone problem might arise from such other candidates.

5.2. Dispersion From Modeled Isolated Source Experiment

Local concentration of biomass burn elements can occur above and in the vicinity of the burns. Such concentration can eventually be advected by the prevailing winds toward the tropical South Atlantic Ocean. This notion is explored in this section using somewhat simple sustained source-based advection experiments using the global model as a frame of reference. The advections, as before, are based on the forecasts covering the period October 12–18, 1992.

Here we shall discuss the results for the following three experiments: a sustained source placed over the burn area of South America; a sustained source in the stratosphere over the southern hemisphere; and a sustained source over the burn region of Africa. These sources are defined in Table 2. It should be noted from Table 2 that the nature of these sources is akin to vertical plumes that provide a continuous supply of tracers. These are being advected by the motion field of the global model. These sources were introduced over a certain vertical depth (Table 2) of the atmosphere over the prescribed location (Table 2). Table 2 also describes the weights that were assigned to the different vertical levels where the sustained source was introduced. The geometries of these sources were either circular or elliptical (Table 2). The maximum strength S of the sustained source was kept at 4 DU/100 mbar layer for each of the three experiments. The horizontal intensity variation of the sustained source is defined by a bell-shaped function.

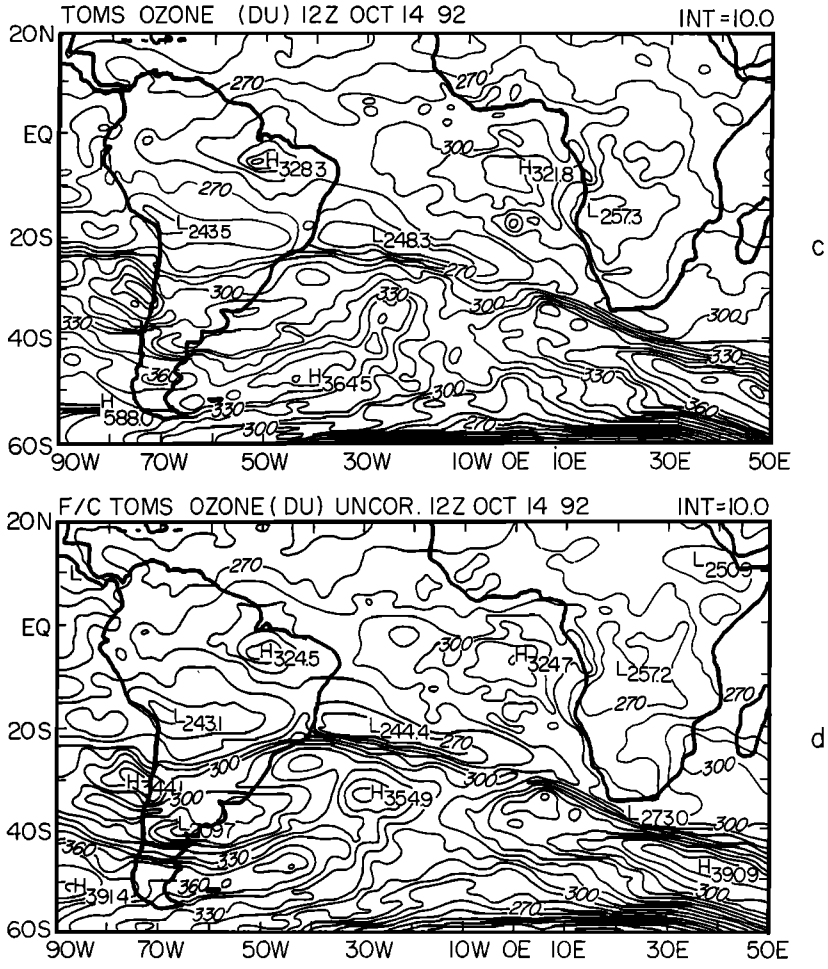

Figure 2. (continued)

$$O_3 = \left(\frac{D^2 - R^2}{D^2 + R^2}\right) S \quad R < D$$

$$O_3 = 0 \quad R \geq D$$

where D is a parameter that defines the lateral size of the source in degrees latitude-longitude, R is the transformed distance from the central point of the source (see Table 2), and S is the maximum sustained ozone concentration.

The rationale for the selection of these sustained sources is the following: the stratospheric sustained source was based on an examination of TOMS data for the week preceding October 14, where we noted a quasi-stationary ozone maximum over the Atlantic coast of South America near 30°S. The source of this maximum appeared to be stratospheric, since its earlier time history showed a passage to that region from much farther south of 25°S. On that basis it was decided to introduce a source near 25°S and 45°W with the specifications described in Table 2. The choice of the other two sustained source regions over South America and Africa were dictated by the mapping of the fire counts. These are illustrated in Plate 2 and Figure 4. The sustained source is introduced almost directly over the burn areas for both of these experiments. The vertical structure of the source (shown in Table 2) reflects plausible vertical distributions that might arise from effects of cumulus convection, which the biomass burn provides vertically. Given a prescribed vertical distribution (Table 2) over the burn regions, the global model is used to carry out a four-dimensional passive tracer advection for each case separately.

A sustained biomass burn source is placed over Africa, between 300 and 900 mbar (Table 2), with a maximum amplitude of 4 DU per 100 mbar. The plume from this source disperses westward very effectively, illustrated in Plate 3 for 700 mbar. In the initial 24 hours some dispersion to the east and west occurs from the predicted winds of October 12 and 13, 1992. The westward dispersal is carried out by the easterlies all the way across the Atlantic Ocean in 3 days. *Jacob et al.* [this issue] emphasized that biomass burning over Africa, a major source of NO_x, undergoes oxidation in the tropical Atlantic basin. The model calculations presented in this paper generally support the possibility of transport in the direction of mean advections, i.e., from Africa to the tropical southern Atlantic Ocean. The computations also suggest that the burn products could be carried toward north central Africa, as well, from the sustained burn region. The predicted motion field does have strong upward motions over the equatorial African belt. Although no sustained source was placed at higher levels, these vertical motions are very effective in carrying the burn products to the 200-mbar level, and these too find their way across the tropical Atlantic in a matter of 1 week (Plate 4). It should be stated that vertical advections appeared to be equally as important as horizontal advections in the eventual shaping of these dispersion patterns. The biomass elements carried up to 200 mbar

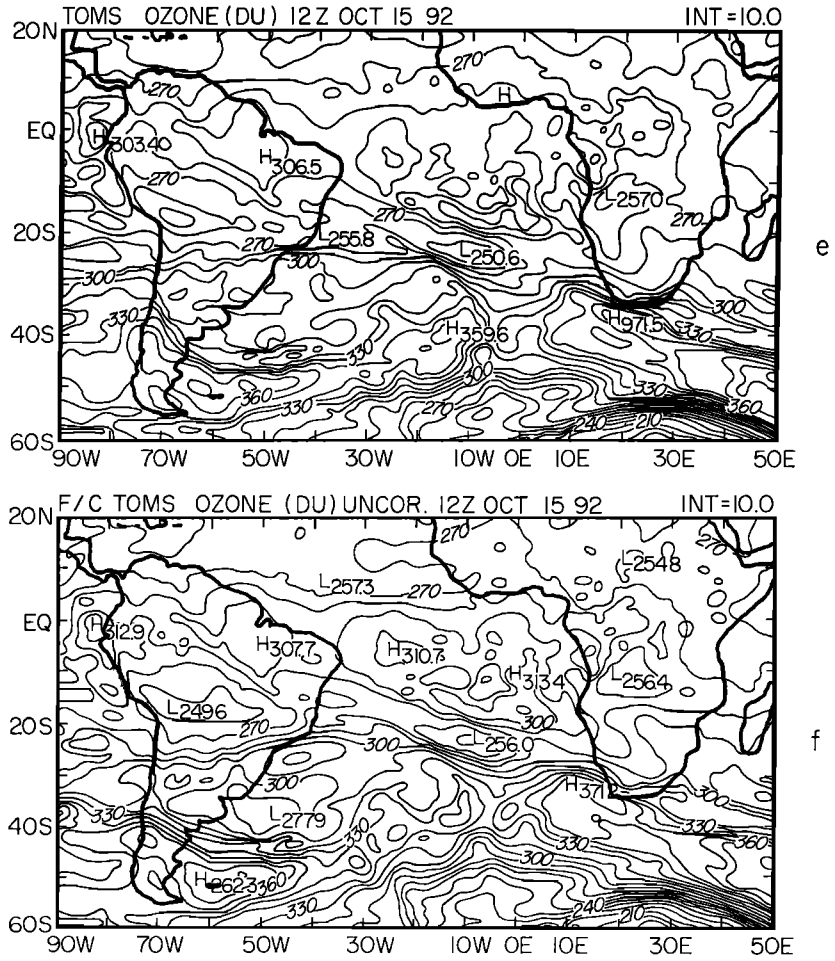

Figure 2. (continued)

appear to execute a counterclockwise advection pattern over the eastern Atlantic Ocean. We also note that this advection pattern includes biomass elements that were first carried upward by tropical convection over central Africa and advected counterclockwise subsequently. This stream of maxima of the advected biomass elements is located in the close proximity of the region of maximum upper tropospheric ozone seen from the ultraviolet differential absorption lidar (UV DIAL) cross sections for October 18, 1992 [*Browell*, 1989]. These maxima values of upper tropospheric ozone of the eastern Atlantic during TRACE A may have had their origin from the burn regions of Africa (Plate 2).

Next we shall illustrate the dispersal from a stratospheric source of the southern hemisphere, between the 100- and 200-mbar surfaces. Plate 5 illustrates the dispersal, at 200 mbar, from this sustained source (Table 2). Westerly winds rapidly disperse the ozone toward West Africa and south of South Africa. A transient anticyclone in the middle of the southern Atlantic Ocean effectively transports ozone equatorward. Since the forecasts of the motion field were fairly accurate up to 6 days, these advective transports, unlike the single trajectories that followed, appear to present a reasonable perspective on the effects of transports. This computation suggests that a steady descent of air can provide a rich source of stratospheric air all the way across the Atlantic Ocean in a matter of 1 week. The choice of the maximum value of 4 DU per 100 mbar is certainly arbitrary. It can be scaled to any desired value, and the advection pattern can be handled accordingly. The descending motion over the source region is reflected in the time history of the evolution of ozone at 400 mbar. Initially, no sustained source was present at 400 mbar (Plate 6). Hence that panel is blank. With time, descent occurs all along the path of the 200-mbar flow toward West Africa. It is this descending flow that appears to be most interesting in contributing to ozone anomalies in the tropical southern Atlantic region at the 400-mbar level. The axis of the 400-mbar advection toward West Africa is not located exactly below that of the 200-mbar plume; the differential horizontal advection produces these features. The descent describes a southern stream at 400 mbar that moves eastward over South Africa. It is also interesting to note that a rather well marked sustained maximum value resides over the east coast of South America at 400 mbar. That was a region of sustained descent in the predicted circulation patterns between 200 and 300 mbar. Such sustained vertical motion features can advect stratospheric air into the tropical upper troposphere in a matter of a few days. However, this may not be crucial for our overall understanding of the ozone anomalies of the tropical southern Atlantic Ocean.

Next we shall illustrate the dispersal from a sustained source over the burn region. These were introduced between 300 and 900 mbar (Figure 4) over Brazil. Its initial geometry at 900 mbar is shown in Plate 7 at hour 0. A steady horizontal plume

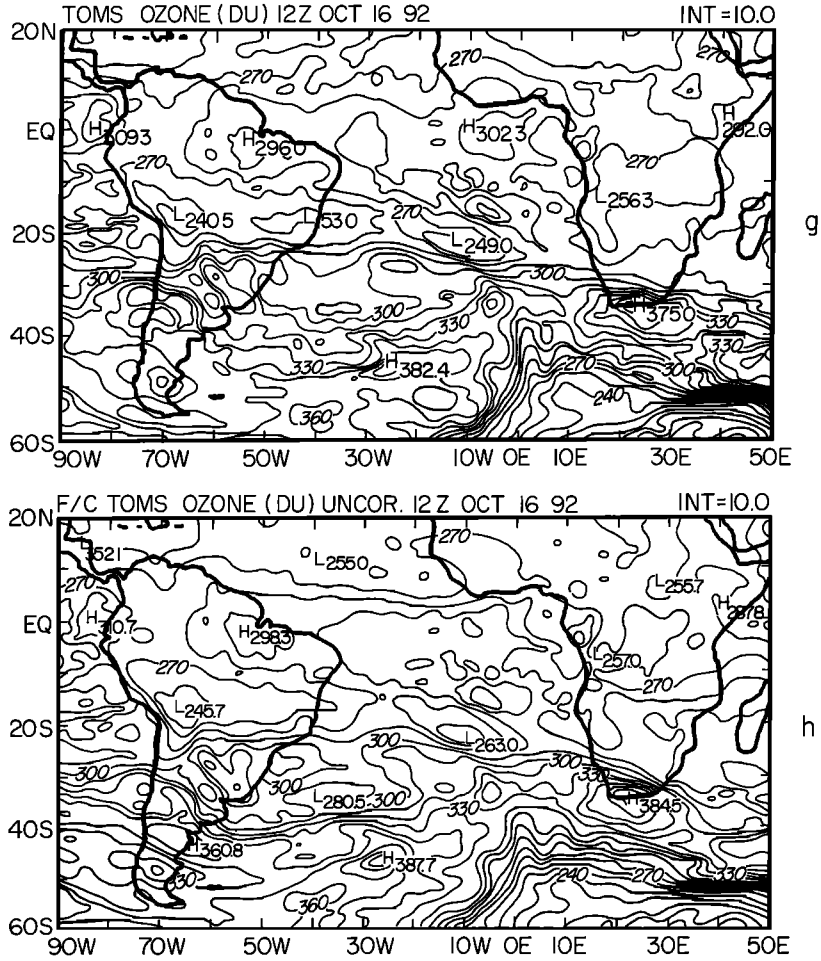

Figure 2. (continued)

extends toward West Africa by day 4. The plume is partly governed by the horizontal advection at 900 mbar but is also affected by the descent from the upper levels because vertical advection over the burn region of Brazil is able to convey the burn elements to upper levels, where stronger westerlies (south of the Intertropical Convergence Zone (ITCZ)) are able to carry them eastward. The plume is also influenced by ensuing descending motions, thus contributing to the extended horizontal plumes at 900 mbar. The scenario at 300 mbar is shown in Plate 8. These burn elements acquire a swath extending toward South Africa and West Africa. The burn elements at 300 mbar make their way toward the Brazilian east coast, where they enter an anticyclonic eddy over the central Atlantic Ocean and eventually exit this domain over South Africa. Overall, the clear impression we get is that a lower tropospheric sustained source over the burn region of South America can contribute to the accumulation of ozone over the tropical southern Atlantic Ocean and describe the transport toward the Indian Ocean as well. A period of roughly 4–6 days is all it takes for communication between the burn regions of Brazil and the tropical southern Atlantic Ocean.

5.3. East-West Circulations and Tropospheric Ozone

Krishnamurti et al. [1993] and *Jacob et al.* [this issue] have emphasized the role of divergent circulations as a possible candidate for contributing to the slow accumulation of ozone over the tropical southern Atlantic Ocean. In this section we shall illustrate the effect of imposing a sustained source in the Asian monsoon around 10°N from where the divergent circulations trace their way to the southern tropical Atlantic Ocean. Figure 5 illustrates the 7-day mean velocity potential at 200 mbar during the period October 12–18, 1992. This illustration clearly portrays the monsoonal teleconnection. Rising motions over the monsoon activity find their compensating descent over equatorial Africa and the tropical eastern Atlantic. We have also examined what would happen to a sustained source of a passive tracer if placed in the vicinity of the monsoonal divergent outflow regions. (See Table 2 for further details on the location, extent, and intensity of this sustained source.) Plate 9 shows the time history of the evolution of a tracer at 200 mbar. A part of this evolution is westward near 10°N from the sustained source. As this tracer moves westward, it makes a counterclockwise, i.e., anticyclonic loop around the eastern tropical Atlantic Ocean. All this time, a gradual descent, carried out by vertical advection, brings this tracer to various upper tropospheric levels. Plate 10 shows its time history at the 300-mbar level. A marked vertical convergence of flux near 300 mbar was also noted in the computations, offering the suggestion that the ozone maximum we noted during TRACE A flights near 9 km above sea level could, in part, be ascribed to the monsoonal east-west teleconnections. In 6 days some of the tracers from the monsoon do appear to reach the lower troposphere over Africa, but the substantial effect is felt at 500 mbar and higher,

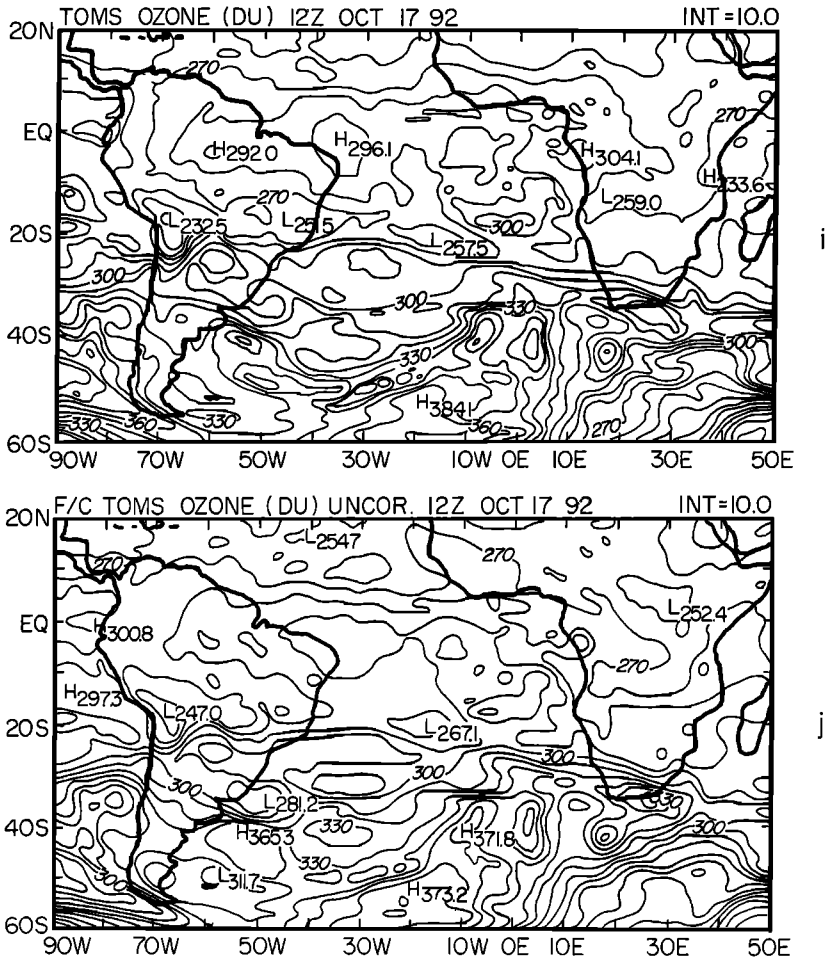

Figure 2. (continued)

where it reaches the tropical southern Atlantic Ocean in 6 days of traverse from the monsoon. *Jacob et al.* [1995] drew several major conclusions from their analysis of the photochemical modeling of the aircraft data during the TRACE A experiment. They concluded that the stratosphere was not important in its contribution to the tropospheric ozone over the tropical southern Atlantic Ocean. They emphasized the role played by the Walker circulation (the Asian monsoonal teleconnections) as important in providing the photochemical reaction for the generation of tropical ozone.

5.4. Optimizing Biomass Burn Sources Toward the TRACE A UV DIAL Cross Section

During the field phase of TRACE A, the NASA DC 8 flew several important chemistry missions (e.g., J. D. Bradshaw et al., How TRACE A compares with other GTE programs: Questions still remaining, submitted to *Journal of Geophysical Research*, 1995 (hereinafter referred to as B95)). Downward and upward directed UV DIAL were able to provide vertical cross sections along the flight track [*Fishman et al.*, this issue]. Figure 6 shows one such flight track which was flown on October 18, 1992. This flight originated from Windhoek in Namibia and was designed to traverse the general region of the ozone maximum over the tropical equatorial Atlantic Ocean.

Figure 7 illustrates a UV DIAL cross section of ozone along the entire flight track of Figure 6.

A goal of this study is to construct and compare the space-time cross section from the various runs of the global model along this "observed" UV DIAL cross section and to see the extent to which similar features can be modeled from the advection of passive tracers.

This UV DIAL cross section of ozone in general appears to describe two maxima, one roughly around 2 km above the ocean and the other located near 9 km. Maximum values of ozone range from roughly 80 to 90 ppbv at these altitudes. A relative minimum value (55 ppbv) may be seen near the 5- to 6-km level and appears to describe the picture over the first three quarters of the flight leg. The last one quarter leg exhibits some differences. The upper tropospheric maximum appears to descend to roughly the 5- to 6-km level with a somewhat complex vertical structure. This UV DIAL based flight cross section of ozone was obtained from tabulations of a more detailed cross section based on the study of B95.

The tabulation at the vertical discretization of the global model leads to some smoothing of the details seen by the UV DIAL ozone observations, which evidently has a much higher resolution (≈0.3 km), whereas the global model tabulation resolves it at a vertical separation of roughly 2–4 km. In spite of this smoothing, the salient features of the UV DIAL ozone cross section shown by B95 are indeed captured in Figure 7a. The corresponding results of the 6-day forecast from the simple passive tracer advection of ozone are shown in Figure 7b. This corresponds to the experiment discussed in section 5.1.

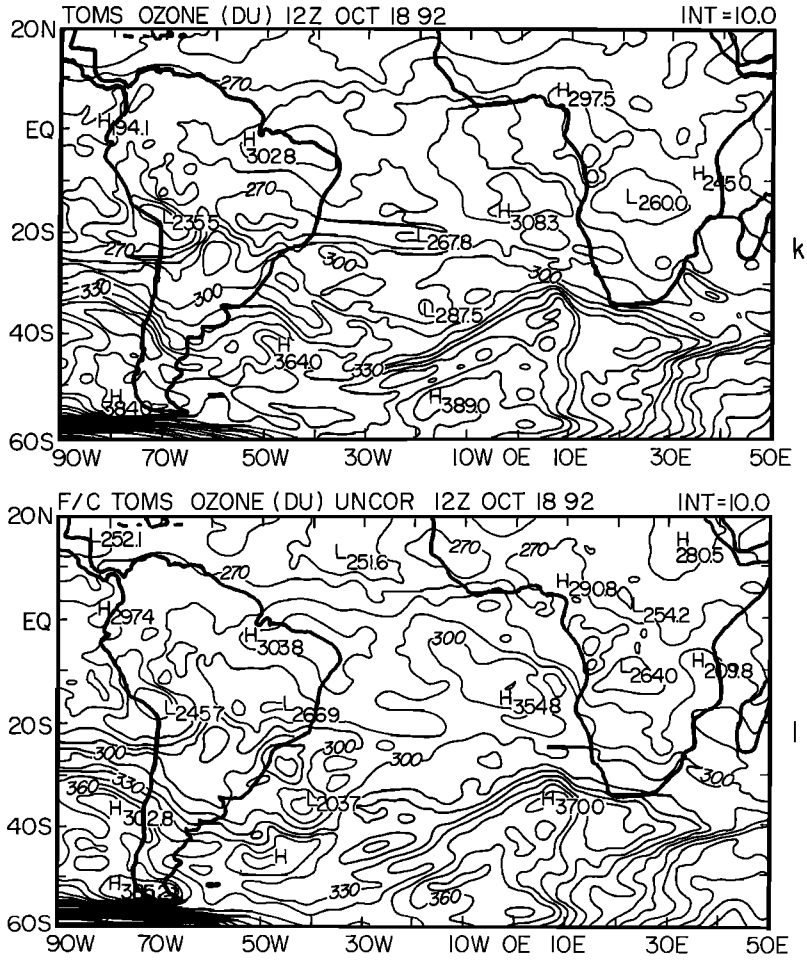

Figure 2. (continued)

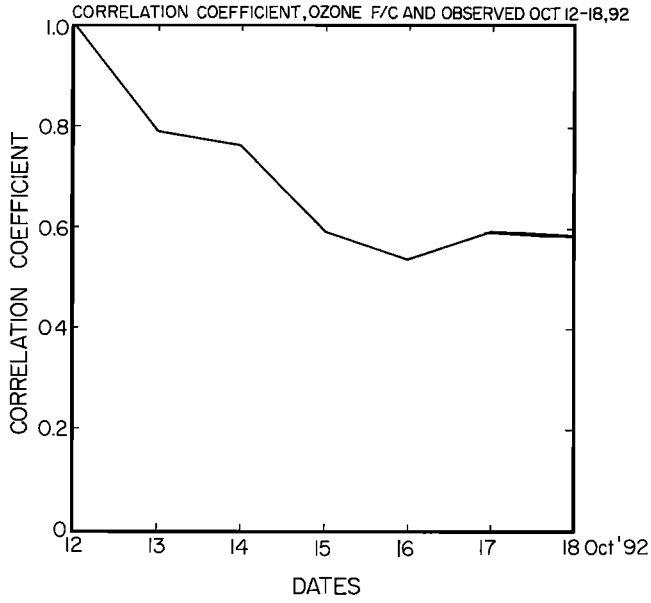

Figure 3. Correlation of observed (TOMS) versus predicted ozone for the 6 days of forecast. Date along abscissa.

We find that although some general agreement with respect to the upper tropospheric ozone maximum is noted here, we find a general decrease of ozone as we proceed down toward the Earth's surface in this model simulation. This reflects a rather smooth representation, lacking an adequate vertical structure of ozone, as is seen in the UV DIAL based cross section (Figure 7a). In order to obtain these results, shown in Figures 7a and 7c, we had to impose the biomass burn tracer patterns that are shown in Figure 8. This was obtained from trial and error through forward and backward integration of the model, keeping in perspective the firecount regions and the UV DIAL ozone concentrations. Figure 8 illustrates, at three selected levels, these burn anomalies of ozone. The results from a 6-day forecast for this experiment are shown in Figure 7c. This compares very well with the UV DIAL based "observed" cross section shown in Figure 7a. The success of this run depended on the location and intensity of the tracers introduced above and in the vicinity of the burn region.

Those initial anomalies, determined via trial and error, were not entirely unreasonable, since the value of total ozone near the burn region was very close to the extrema of the ozonesonde values during October 1992 over Brazzaville, Ascension, and Natal. The comparison of the modeled ozone (Figure 7c)

Table 2. Sustained Sources

Serial Number	Source	Central Position of Source	Vertical Extent, mbar	Vertical Weighting Factors	Horizontal Extent*		
					α	β	D
1	Stratosphere	25°S, 45°W	100	1.0	1.0	1.0	11.0
2	Brazil	7.5°S, 42.5°W	300–900	1.0 everywhere	1.0	6.0	1.0
		5.0°S, 55.0°W	300–900	1.0 everywhere	0.4	6.0	1.0
3	Africa	15°S, 25°E	300–900	1.0 everywhere	0.4	1.0	6.0
4	Monsoon	5°N, 45°E	150	0.5	1.0		5.0
			200	1.0		1.0	
			250	0.5			

*$R < D$; $R = [(\alpha\Delta\lambda)^2 + (\beta\Delta\theta)^2]^{1/2}$

and the observed ozone (Figure 7a), is plotted in vertical cross sections, and their comparison with the no burn ozone cross section (Figure 7b) suggests that in order to describe the ozone and its vertical structure over the tropical southern Atlantic, we need to invoke tracer elements from the biomass burn regions. If these are done carefully, we can make dramatic improvements in the simulation. The procedure we have adopted here is no more than an intermediate step toward the eventual photochemical modeling that is desirable.

6. Limitations of Present Work

There are several areas where further improvements in the present work are needed.

1. A higher resolution global model is needed for the simulation of vertical stratification of ozone, seen in the aircraft-based UV DIAL cross sections. The details of the UV DIAL based airborne UV DIAL ozone are displayed as vertical averages over distances of the order of 300 m. Thus we see a lot

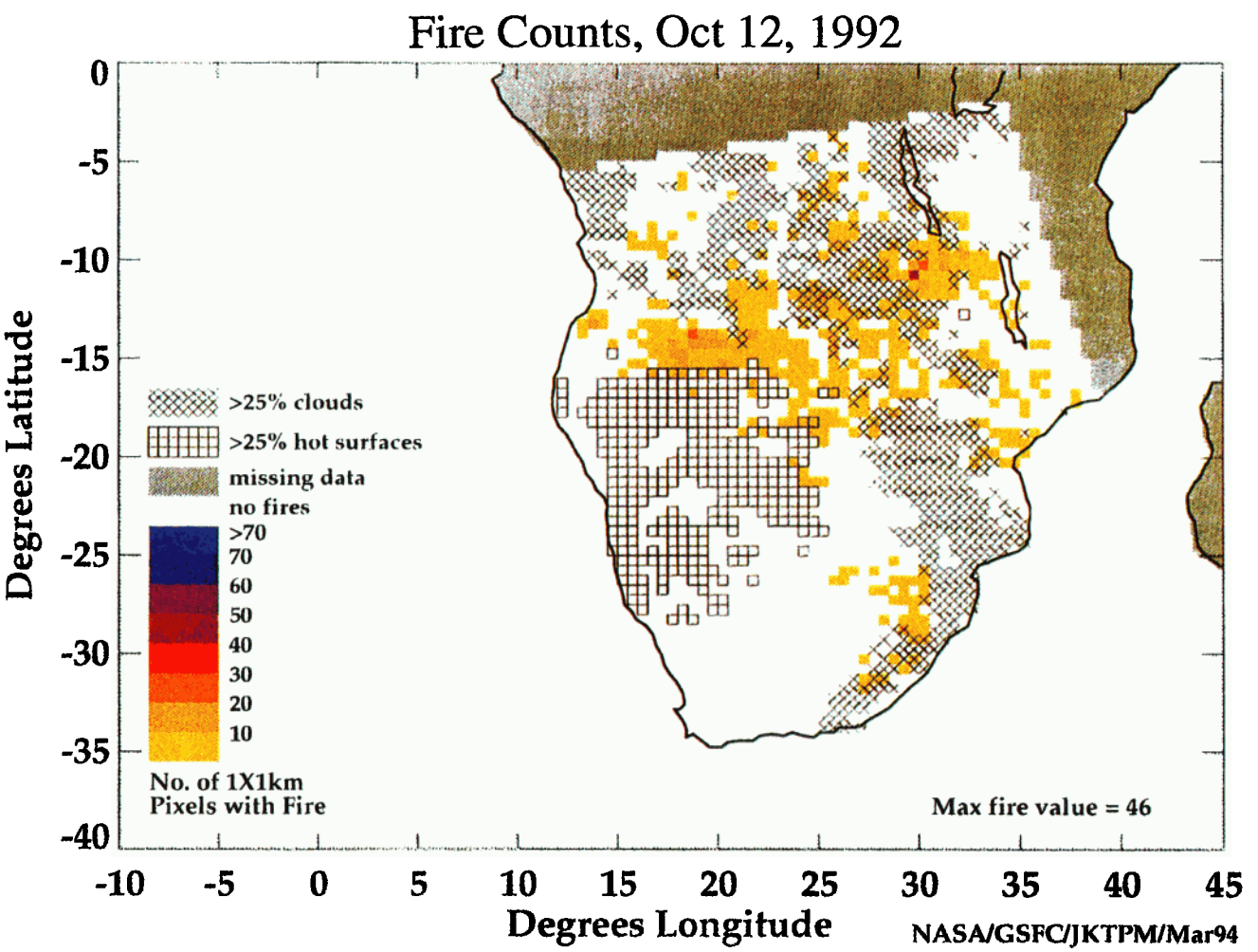

Plate 2. Fire count data provided by NASA Goddard for South Africa; October 12, 1992 (number of 1 × 1 km pixels with fire).

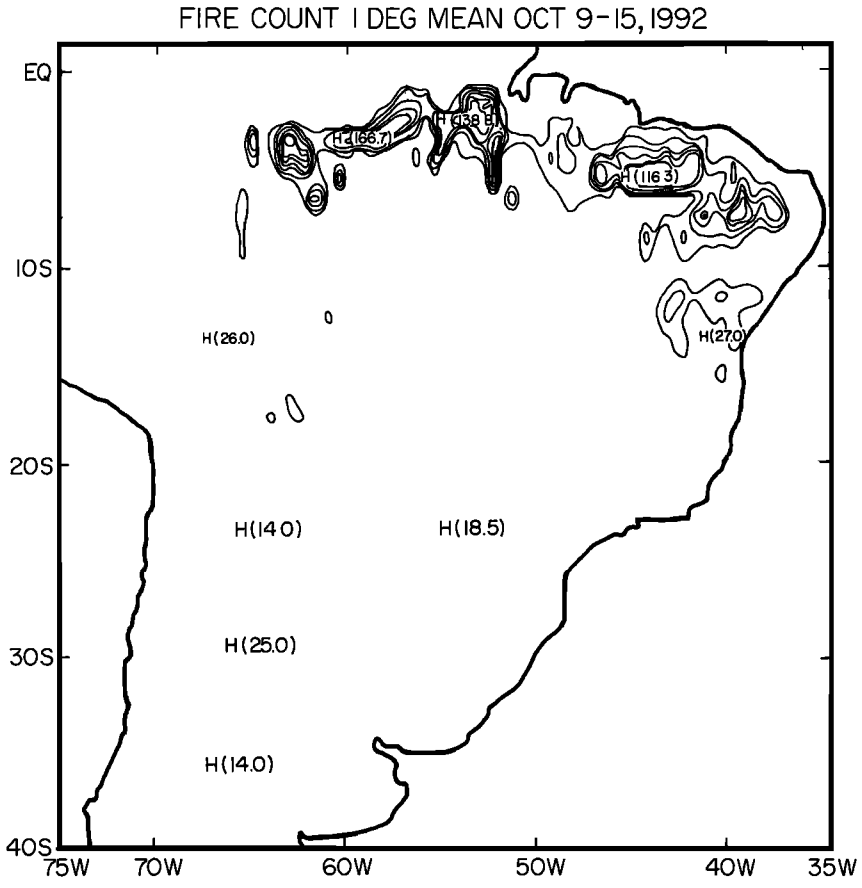

Figure 4. South America fire count 1° mean, October 9–15, 1992.

of detail in these measurements that the model with a vertical resolution of around 2–4 km fails to resolve.

2. All our experiments are based on the premise of passive transports. We do not allow for any short-period changes that may arise from photochemical processes.

3. In the use of TOMS as a basic data set for the total ozone, we have not included any of the corrections that have been highlighted by *Thompson et al.* [1993] and *Kim et al.* [this issue]. These are needed refinements that can be done when the corrected TOMS data become more generally available. Moreover, a better structure function will give much more realistic predictions.

4. The semi-Lagrangian advection can be further improved to meet the requirements of higher resolution details.

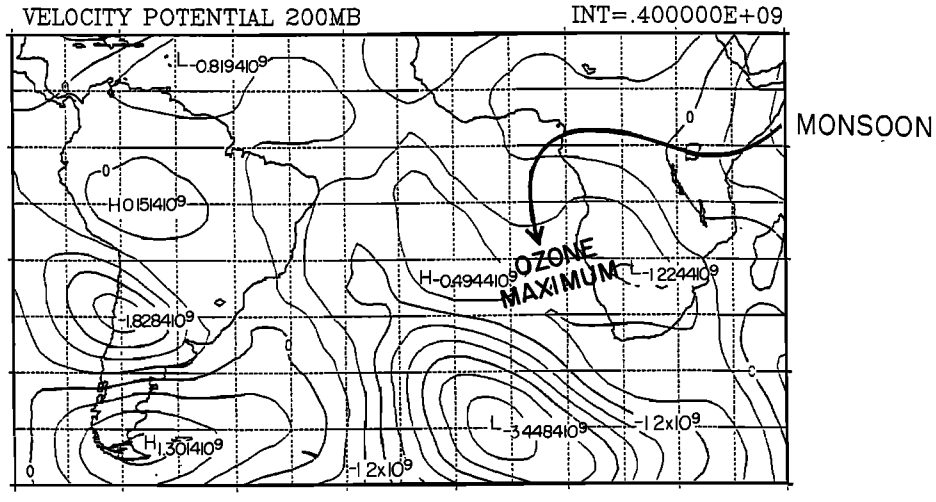

Figure 5. Velocity potential at 200 mbar (through solid lines) for the period of integration. Intervals are 4 $\times 10^8$ m^2 s^{-1}. The heavy solid line shows the divergent flow teleconnection with the monsoon.

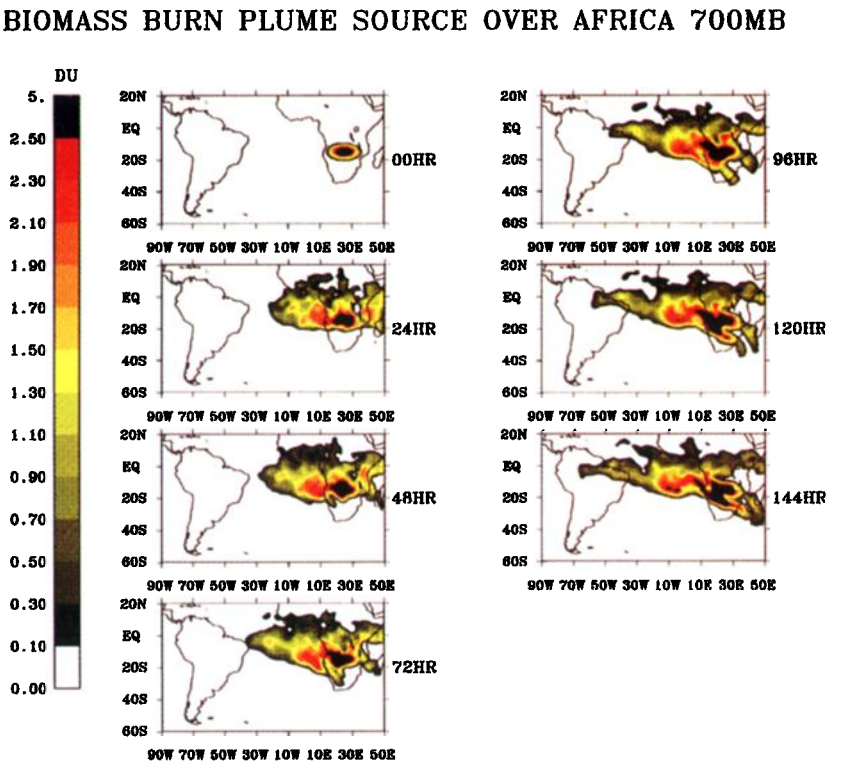

Plate 3. Biomass burn (sustained source) over Africa (details in Table 2). The panels show the 144-hour history of dispersion at 700 mbar. Units are DU/100 mbar.

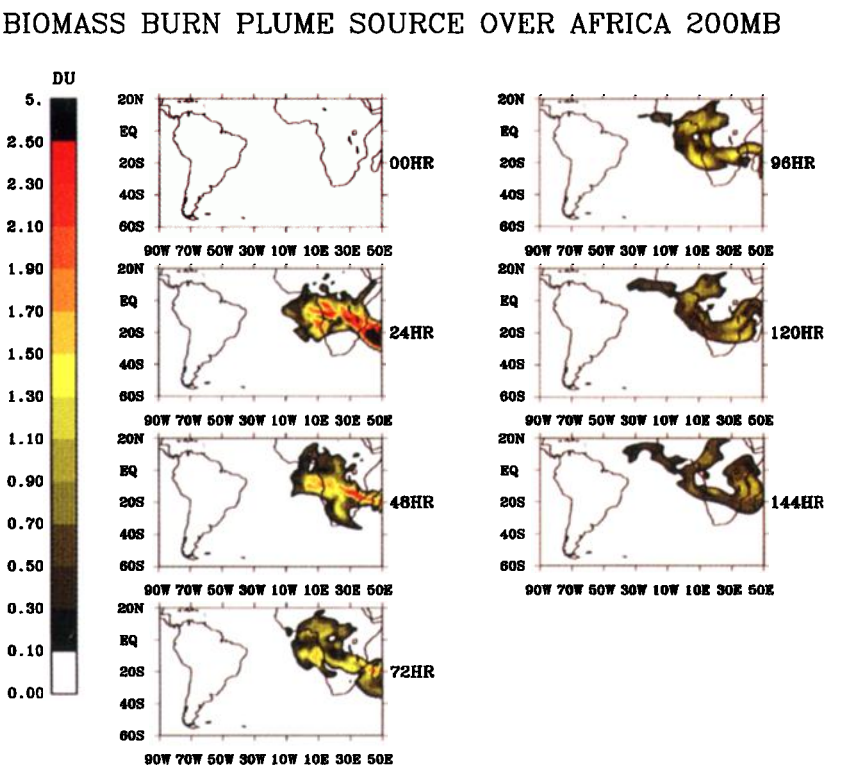

Plate 4. Same as Plate 3, illustrating the dispersal at 200 mbar.

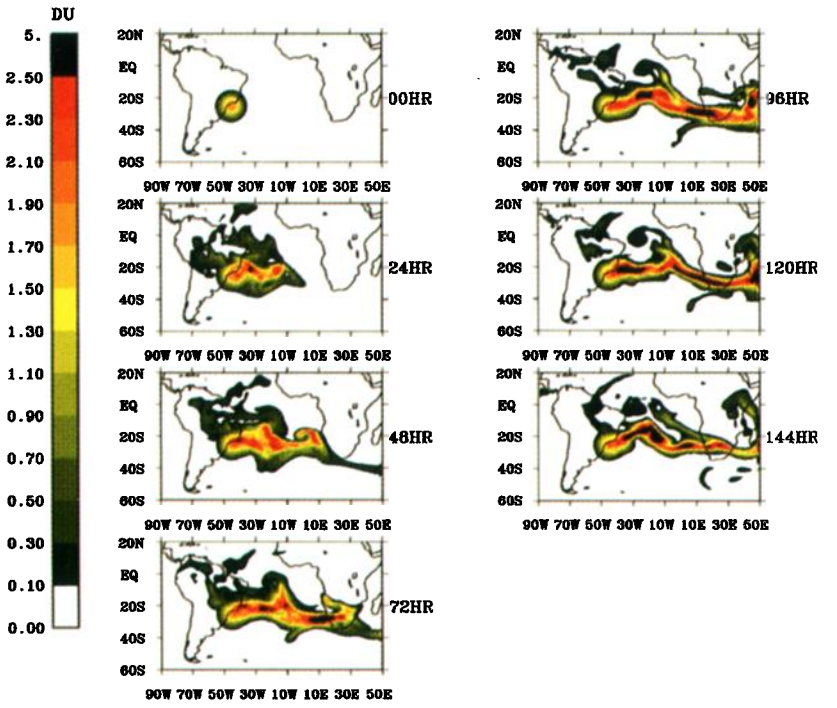

Plate 5. Stratospheric sustained sources over the South American coast (details in Table 2). The panels illustrate the 144-hour history of dispersal at 200 mbar. Units are DU/100 mbar.

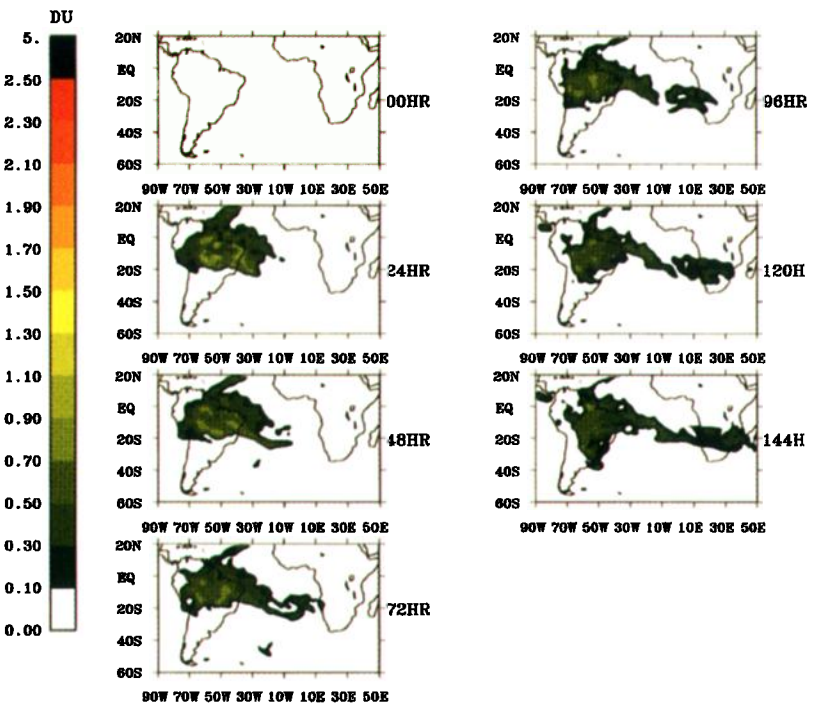

Plate 6. Same as Plate 5, illustrating the dispersal at 400 mbar.

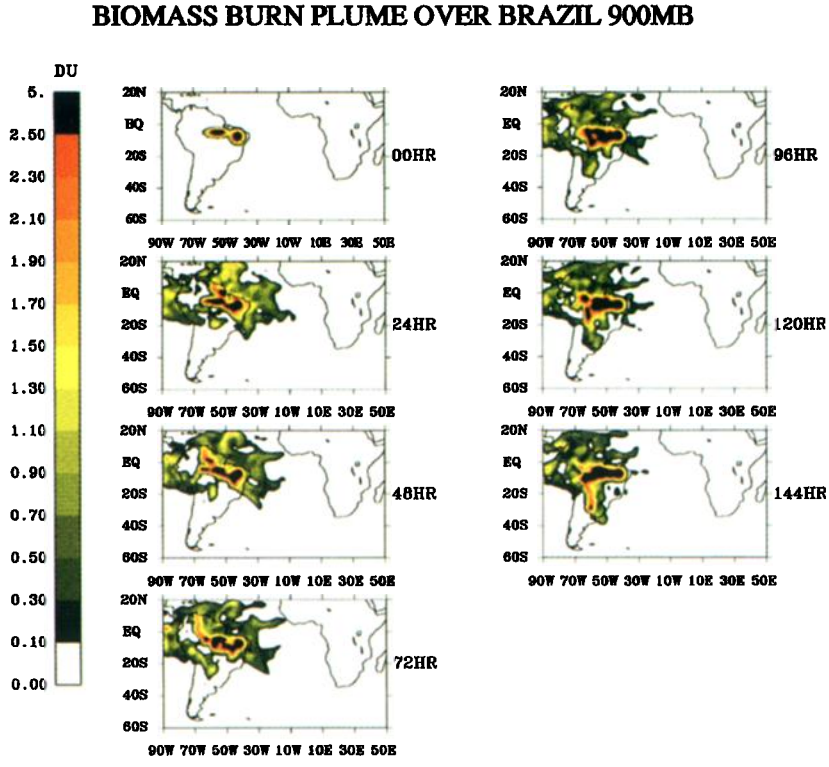

Plate 7. Biomass burn (sustained source) over Brazil (details in Table 2). The panels show the 144-hour history of dispersal at 900 mbar. Units are DU/100 mbar.

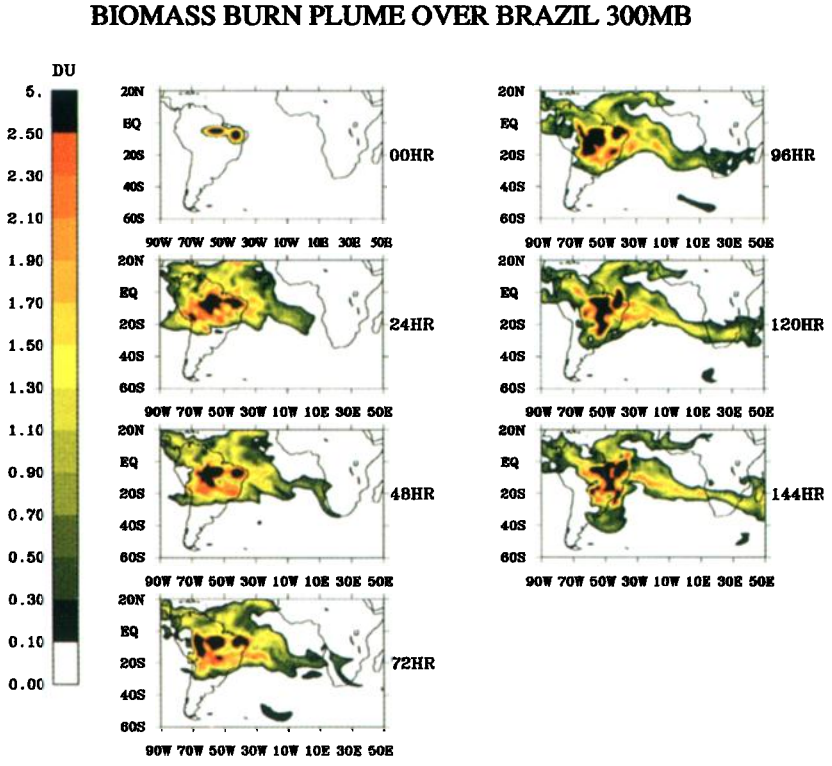

Plate 8. Same as Plate 7, illustrating the dispersal at 300 mbar.

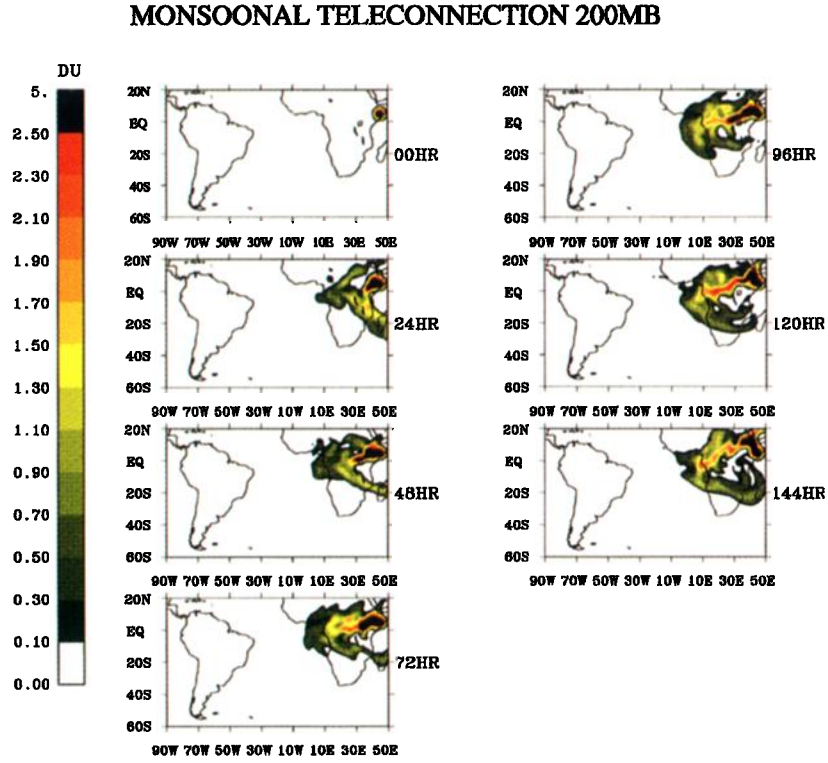

Plate 9. The 200-mbar sustained source over the northern Arabian Sea (details in Table 2). Panels illustrate the 144-hour history of dispersal at 200 mbar. Units are DU/100 mbar.

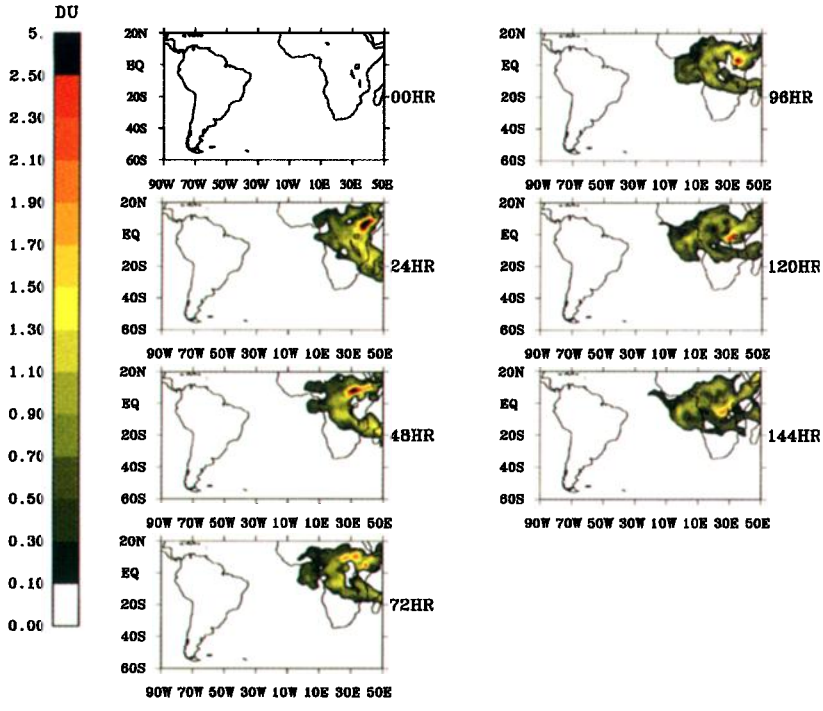

Plate 10. Same as Plate 9, illustrating the dispersal at 300 mbar.

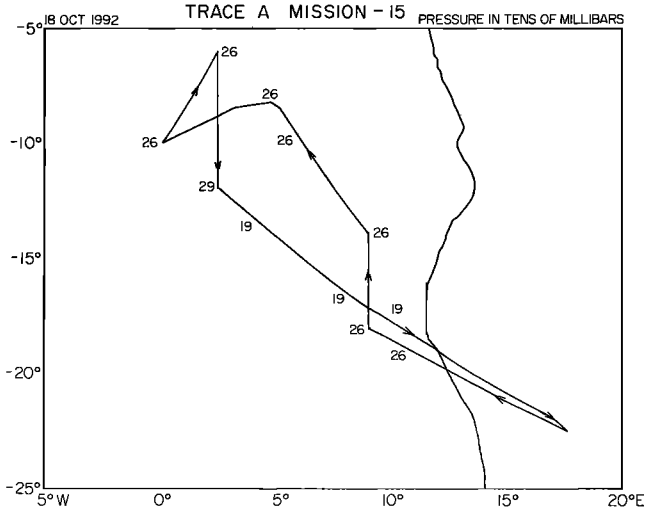

Figure 6. Aircraft flight track for October 18, 1992. Flight track pressure shown in tens of millibars. UV DIAL cross section was made all along this flight track.

7. Concluding Remarks

The most striking result of this study is that we are able to demonstrate skills of the order of 0.8 (correlations of observed TOMS versus model-based estimates of ozone over the larger TRACE A domain) for the prediction of total ozone as a passive tracer for periods of the order of 1 week without recourse to photochemistry. The results presented here for the dynamics alone experiments may be dependent on the choice of the initial structure function. Further experimentation is needed to explore sensitivity in this area.

Dynamics alone models, which are based on transports of passive tracers, do not generate the fine structures of vertical distributions of ozone as are seen in the reconnaissance aircraft based UV DIAL measurements. There exists an obvious mismatch in the scales of UV DIAL observations and the global model's horizontal and vertical resolution. As a consequence, it is not possible to make a one-to-one comparison. We had resorted to a filtering of the smaller scales of the UV DIAL data. Insertion of biomass sources in the model integration appears to provide a vertical fine structure in the forecasts, something that was not possible from the so-called dynamics alone experiments. There is a need to refine the dynamics alone model further, i.e., to incorporate some measure of the photochemistry. The fine structure one sees in the ozonesonde data from Brazzaville, Ascension, and Natal and from the UV DIAL observations of ozone over the tropical Atlantic are perhaps revealing of the biomass burn contributions.

By carrying out a large number of sustained source experiments, we have shown that, in the time frame of 1 week, the tropical southern Atlantic Ocean can experience the accumulation of ozone from sources introduced over the African burn regions, Brazilian burn regions, southern hemisphere stratosphere, and monsoonal east-west circulations. These experiments show that both horizontal and vertical advective processes play equally important roles in the eventual dispersal and shaping of ozones over the tropical southern Atlantic Ocean. Burn elements in the lower troposphere over Africa and South America are transported upward by atmospheric vertical motion and also laterally advected by upper winds. The

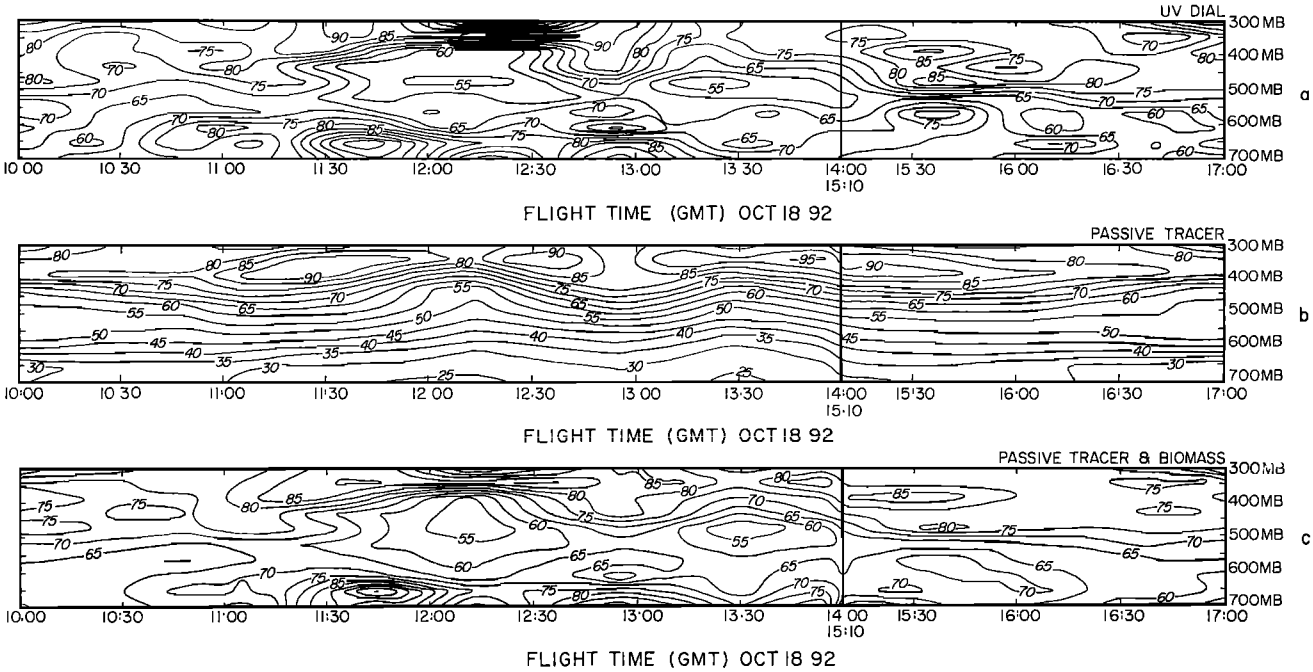

Figure 7. (a) UV DIAL ozone cross section (interpolated to the vertical levels of the global model) along the flight track of Figure 6. Units are ppbv. (b) Model-based (6-day forecast) cross section of ozone along the flight track of Figure 6 from a passive tracer experiment. Units are ppbv. (c) Model-based (6-day forecast) cross section of ozone along the flight track of Figure 6 obtained from an experiment that includes optimized biomass burn sources over Africa and Brazil. Units are ppbV.

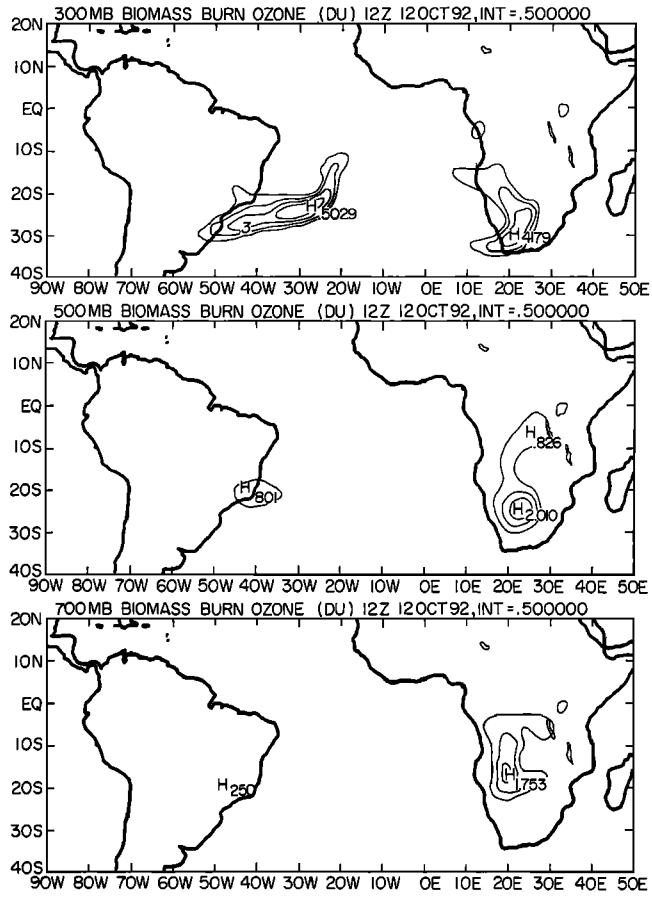

Figure 8. Initial configuration of biomass burn tracers introduced to improve modeling over the region of the UV DIAL cross section of Figure 7a at (a) 300 mbar, (b) 500 mbar, and (c) 700 mbar. Units are DU/100 mbar.

resulting geometry of the plumes looks quite similar to what we have noted from the animation of TOMS data over the tropical Atlantic.

A major observational contribution of TRACE A was the airborne UV DIAL measurements of ozone. These provided vertical cross sections of ozone with some definitive vertical structures with maximum ozone near the inversion layer and the upper troposphere of the tropical southern Atlantic Ocean. In order to model such fine features we had to invoke hypothetical tracer geometries over the fire count region of Africa and Brazil. That was done with amplitudes within the ranges of the extrema of ozone from the soundings of ozone at Brazzaville, Natal, and Ascension. It was possible to model the vertical cross sections of ozone along the aircraft track of TRACE A to some reasonable degree.

The dynamics alone experiments are quite revealing and bring out the use of numerical global models for such studies. In fact, the inclusion of explicit photochemistry in the model can provide answers to many unexplained features of atmospheric photochemistry.

Acknowledgments. The data sets for this study came from NASA Goddard, NASA Langley, and the National Meteorological Center in Washington, D. C. Jack Beven assisted in the extraction of high-resolution cloud motion vectors for TRACE A. The research reported here was supported by NASA grant NAG 1-1312. The computations were carried out on the CRAY/YMP at Florida State University.

References

Bachmeier, A. S. and H. E. Fuelberg, Meteorological overview of the Transport and Atmospheric Chemistry Near the Equator–Atlantic (TRACE A) experiment, *J. Geophys. Res.*, this issue.

Browell, E. V., Differential absorption lidar sensing of ozone, *Proc. IEEE, 77*, 419–432, 1989.

Businger, J. A., J. C. Wyngard, Y. Izumi, and E. F. Bradley, Flux profile relationship in the atmospheric surface layer, *J. Atmos. Sci., 28*, 181–189, 1971.

Dütsch, H. W., Vertical ozone distribution on a global scale, *Pure Appl. Geophys., 116*, 529, 1978.

Fishman, J., Experiment probes elevated ozone levels over the tropical South Atlantic Ocean (abstract), *Eos Trans. AGU, 75*(33), 380, 1994.

Fishman, J., C. E. Watson, J. C. Larsen, and J. A. Logan, Distribution of tropospheric ozone determined from satellite data, *J. Geophys. Res., 95*, 3599–3618, 1990.

Fishman, J., F. Fakhruzzaman, B. Cros, and D. Nganga, Identification of widespread pollution in the southern hemisphere from satellite analyses, *Science, 252*, 1693–1696, 1991.

Fishman, J., V. G. Brackett, E. V. Browell, and W. B. Grant, Tropospheric ozone derived from TOMS/SBUV measurements during TRACE A, *J. Geophys. Res.*, this issue.

Fuelberg, H. E., R. O. Loring Jr., M. V. Watson, M. C. Sinha, K. E. Pickering, A. M. Thompson, G. W. Sachse, D. R. Blake, and M. R. Schoeberl, TRACE A trajectory intercomparison, 2, Isentropic and kinematic methods, *J. Geophys. Res.*, this issue.

Harshvardan, and T. G. Corsetti, Longwave parameterization for the UCLA/GLAS GCM, *NASA Tech. Memo., TN-86072*, 1984.

Hilsenrath, E., P. J. Dunn, and C. L. C. Mateer, Standard ozone profiles from balloon and rocket data for satellite and theoretical model input, paper presented at Joint Assembly, Int. Assoc. of Geomagn. and Aeron./Int. Assoc. of Meteorol. and Atmos. Phys., Seattle, Washington, 1977.

Jacob, D. J., et al., Origin of ozone and NO_x in the tropical troposphere: A photochemical analysis of aircraft observations over the South Atlantic basin, *J. Geophys. Res.*, this issue.

Kanamitsu, M., On numerical prediction over a global tropical belt, *Rep. 75-1*, pp. 1–282, Dep. of Meteorol., Fla. State Univ., Tallahassee, 1975.

Kanamitsu, M., Description of the NMC global data assimilation and forecast system, *Weather Forecasting, 4*, 335–342, 1989.

Kanamitsu, M., K. Tada, K. Kudo, N. Sato, and S. Isa, Description of the JMA operational spectral model, *J. Meteorol. Soc. Jpn., 61*, 812–828, 1983.

Kim, J. H., R. D. Hudson, and A. M. Thompson, A new method of deriving time-averaged tropospheric column ozone over the tropics using TOMS radiances: Intercomparison and analysis using TRACE A data, *J. Geophys. Res., this issue.*

Kitade, T., A numerical study of vortex motion with barotropic models, *J. Meteorol. Soc. Jpn., 59*, 801–807, 1981.

Krishnamurti, T. N., S. Low-Nam, and R. Pasch, Cumulus parameterization and rainfall rates II, *Mon. Weather Rev., 111*, 816–828, 1983.

Krishnamurti, T. N., D. K. Oosterhoff, and N. Dignon, Hurricane prediction with a high resolution global model, *Mon. Weather Rev., 117*, 631–669, 1989.

Krishnamurti, T. N., A. Kumar, K. S. Yap, A. P. Dastoor, N. Davidson, and J. Sheng, Performance of a high-resolution mesoscale tropical prediction model, *Adv. Geophys., 32*, 133–286, 1990.

Krishnamurti, T. N., K. S. Yap, and D. K. Oosterhoff, Sensitivity of tropical storm forecast to radiative destabilization, *Mon. Weather Rev., 119*, 2176–2205, 1991.

Krishnamurti, T. N., H. E. Fuelberg, M. C. Sinha, D. Oosterhoff, E. L. Bensman, and V. B. Kumar, The meteorological environment of the tropospheric ozone maximum over the tropical South Atlantic, *J. Geophys. Res., 98*, 10,621–10,641, 1993.

Lacis, A. A., and J. E. Hansen, A parameterization for the absorption of solar radiation in the Earth's atmosphere, *J. Atmos. Sci., 31*, 118–133, 1974.

Louis, J. F., A parametric model of vertical eddy fluxes in the atmosphere, *Boundary Layer Meteorol., 17*, 187–202, 1979.

Pickering, K. E., A. M. Thompson, D. P. McNamara, M. R. Schoeberl, K. Fahkruzzaman, H. E. Fuelberg, R. O. Loring Jr., and M. C. Sinha,

An examination of factors contributing to trajectory uncertainty over the South Atlantic (abstract), *Eos Trans. AGU*, *75*(16), Spring Meet. Suppl., 86, 1994.

Thompson, A. M., K. E. Pickering, D. P. McNamara, and R. D. McPeters, Effects of marine stratocumulus on TOMS ozone, *J. Geophys. Res.*, *98*, 23,051–23,058, 1993.

Thompson, A. M., et al., Ozone over southern Africa during SAFARI 92/TRACE A, *J. Geophys. Res.*, this issue.

Tiedtke, M., The sensitivity of the time-mean large-scale flow to cumulus convection in the ECMWF model, in *Workshop on Convection in Large-Scale Numerical Models*, pp. 297–316, Eur. Cent. for Medium-Range Weather Forecasts, Reading, England, 1984.

R. Chatfield, Earth System Science Division, NASA Ames Research Center, Moffett Field, CA 94035.

H. Fuelberg, T. N. Krishnamurti, D. Oosterhof, and M. C. Sinha, Department of Meteorology, Florida State University, Tallahassee, FL 32306. (e-mail: TNK@cloudl.met.fsu.edu)

D. J. Jacob and J. Logan, Department of Earth and Planetary Sciences, Harvard University, Cambridge, MA 02138.

M. Kanamitsu, National Meteorological Center, W/NMC2, WWB Room 204, Washington, DC 20233.

(Received March 14, 1995; revised July 20, 1995; accepted July 25, 1995.)